Spintronics in low dimensional magnets

Dr. Shang-Fan Lee
Institute of Physics, Academia Sinica

Financial support by Academia Sinica and National Science and Technology Council is acknowledged

Fig. 1: Illustration of 2D magnetic materials, showing the critical temperature and electrical properties.

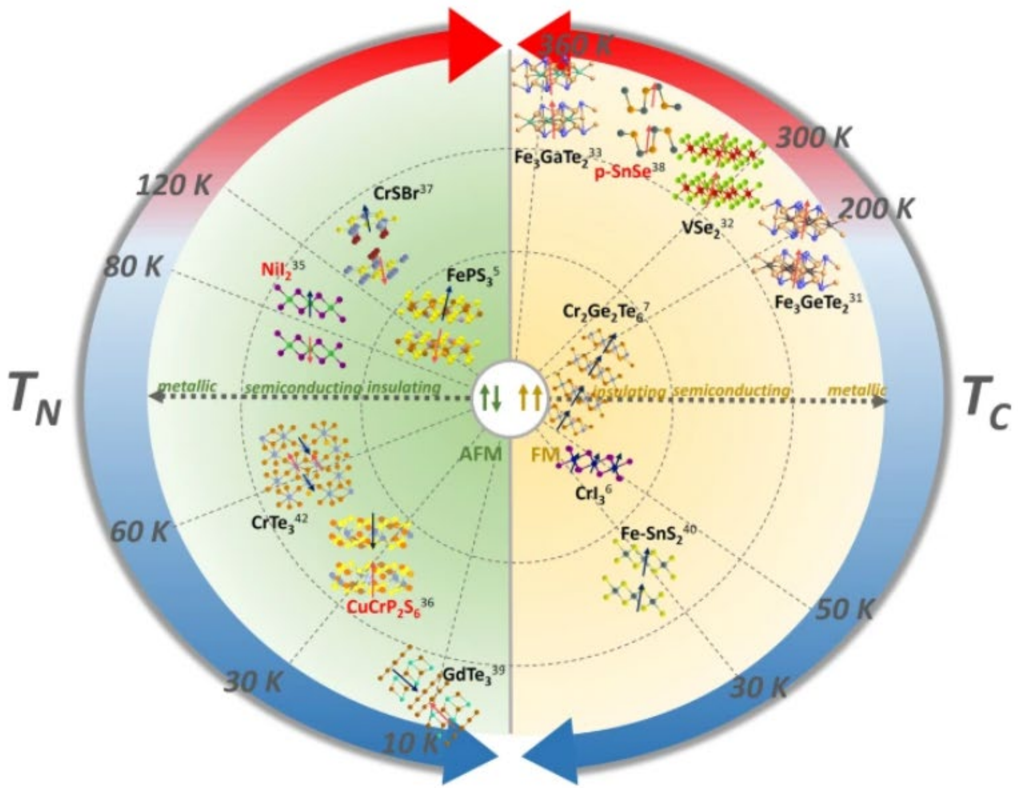

Arrangement is in accordance with their magnetism, conductivity, and critical temperature. Ferromagnetic and antiferromagnetic materials are characterized by Curie and Néel temperatures, respectively. They are divided into three dashed spheres based on conductivity: smallest (insulating), medium (semiconducting), and large (metallic). Multiferroics are highlighted in red color.

Review Article | Open access | Published: 30 May 2024

2D Magnetic heterostructures: spintronics and quantum future

Bingyu Zhang, Pengcheng Lu, Roozbeh Tabrizian, Philip X.-L. Feng & Yingying Wu

npj Spintronics **2**, Article number: 6 (2024) | Cite this article

Introduction

to some major development in spintronics

- Giant Magnetoresistance, Tunneling Magnetoresistance
- Spin Transfer Torque (STT)
- Spin Orbit torque (SOT)
  - Pure Spin current (no net charge current)
    - Spin Hall, Inverse Spin Hall effects
    - Spin Pumping effect
    - Spin Seebeck effect

Two dimensional van der Waals ferromagnets (Fe_3GeTe_2, Fe_3GaTe_2 …) and antiferromagnets ($NiPS_3$, NiI_2 …)

Opportunities:

- Good old physics in new low dimensional materials
- Proximity effect to graphene, bilayer graphene, twisted Moiré patterns …

2007 Nobel prize in Physics

2007 Nobel Laureate in physics Albert Fert and Peter Grünberg)

Giant Magnetoresistance
Tunneling Magnetoresistance

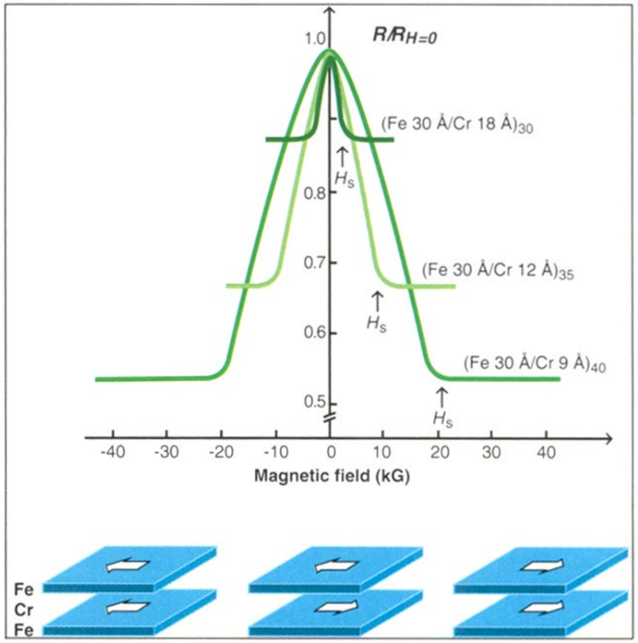

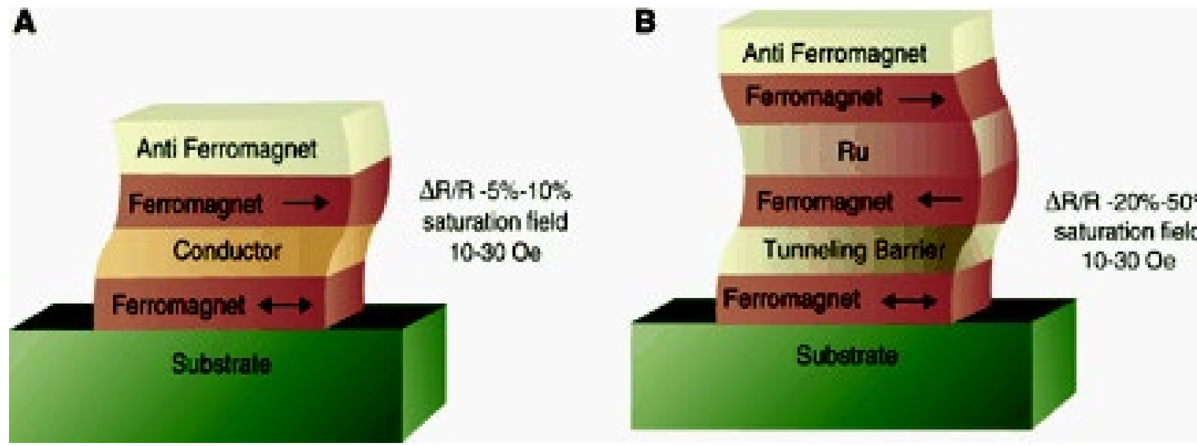

Discovery of Giant MR -- Two-current model combines with magnetic coupling in multilayers

Spin-dependent transport structures. (A) Spin valve. (B) Magnetic tunnel junction. (from Science)

Moodera's group, PRL **74**, 3273 (1995)

Fert's group, PRL **61**, 2472 (1988)

Miyazaki's group, JMMM **139**, L231(1995)

Valet and Fert model of (CPP-)GMR

Based on the Boltzmann equation

A semi-classical model with spin taken into consideration

$$j_{+(-)} = \frac{1}{e\rho_{+(-)}} \frac{\partial \mu_{+(-)}}{\partial x}$$

$$j_{+} + j_{-} = j_e$$

$$\frac{\partial (j_+ - j_-)}{\partial x} = \frac{2eN(E_F)\Delta\mu}{\tau_{sf}}$$

$$\frac{\partial^2 \mu_{+(-)}}{\partial z^2} = \frac{\mu_{+(-)}}{l_{sf}^2}$$

$$l_{sf}^F = \left[\lambda_{sf}^F / 3(\lambda_\uparrow^{-1} + \lambda_\downarrow^{-1})\right]^{1/2}, \quad l_{sf}^N = \left[\lambda_{sf}^N \lambda / 6\right]^{1/2}$$

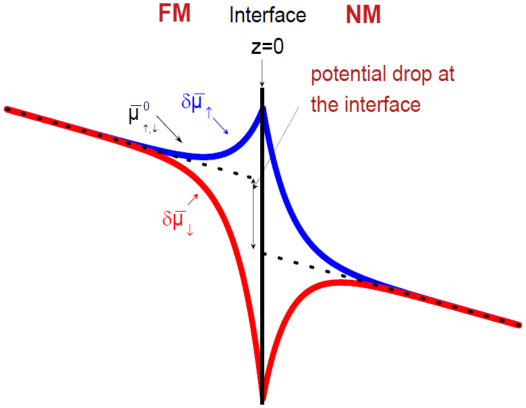

Δμ for antiparallel aligned multilayers

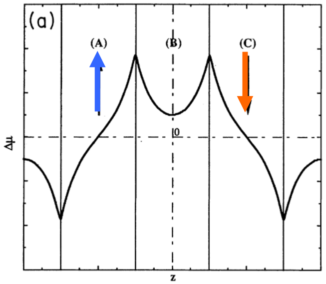

Δμ for parallel aligned multilayers

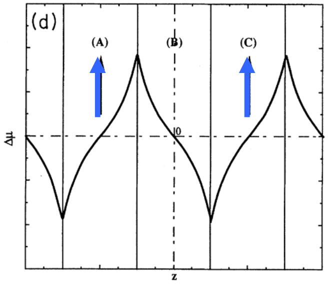

Spin imbalance induced charge accumulation at the interface is important

Spin diffusion length, instead of mean free path, is the dominant physical length scale

Spin Transfer Torque (STT)

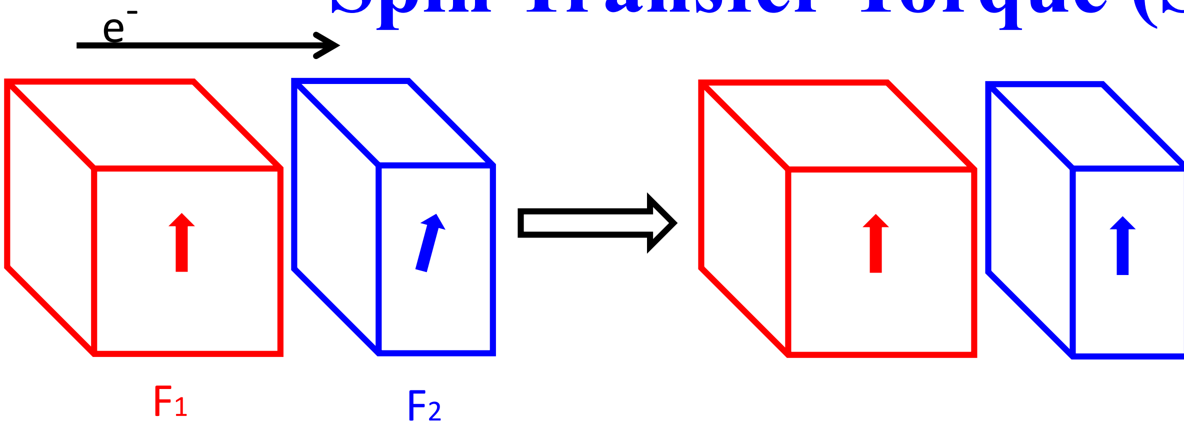

Large current density induces magnetization rotation because of local spin angular momentum conservation

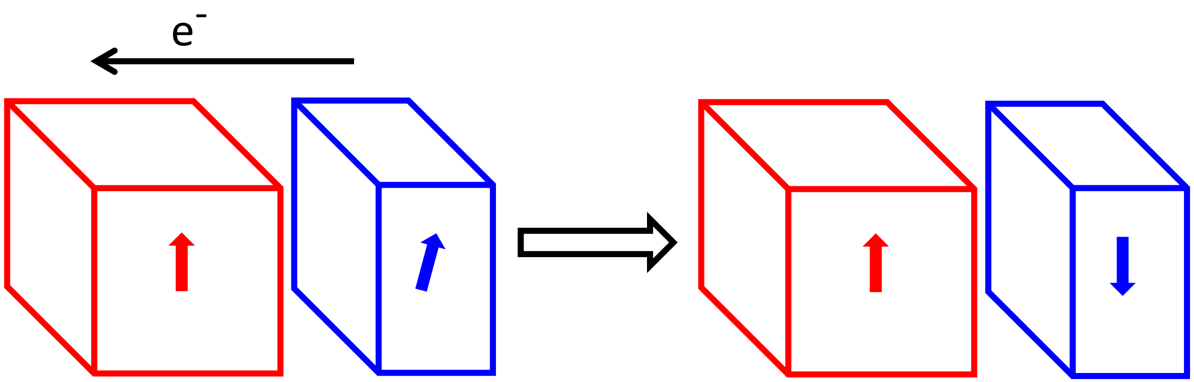

When applied current and external field act against each other, magnetization precession radiates microwave.

In a trilayer, current direction determines the relative orientation of F_1 and F_2 when H = 0.

F_1 is pinned layer. Minority spins are responsible for the antiferromagnetic final state.

Spin Transfer Torque

Landau-Lifshitz-Gilbert equation with Spin Transfer Torque terms

$$\frac{\partial \vec{M}}{\partial t} = -\gamma \vec{M} \times \vec{H}_{\text{eff}} + \frac{\alpha}{M_s} \vec{M} \times \frac{\partial \vec{M}}{\partial t} - \frac{b_j}{M_s^2} \vec{M} \times \left(\vec{M} \times \frac{\partial \vec{M}}{\partial x}\right) - \frac{c_j}{M_s} \vec{M} \times \frac{\partial \vec{M}}{\partial x}$$

$b_j, c_j \sim JP/t$

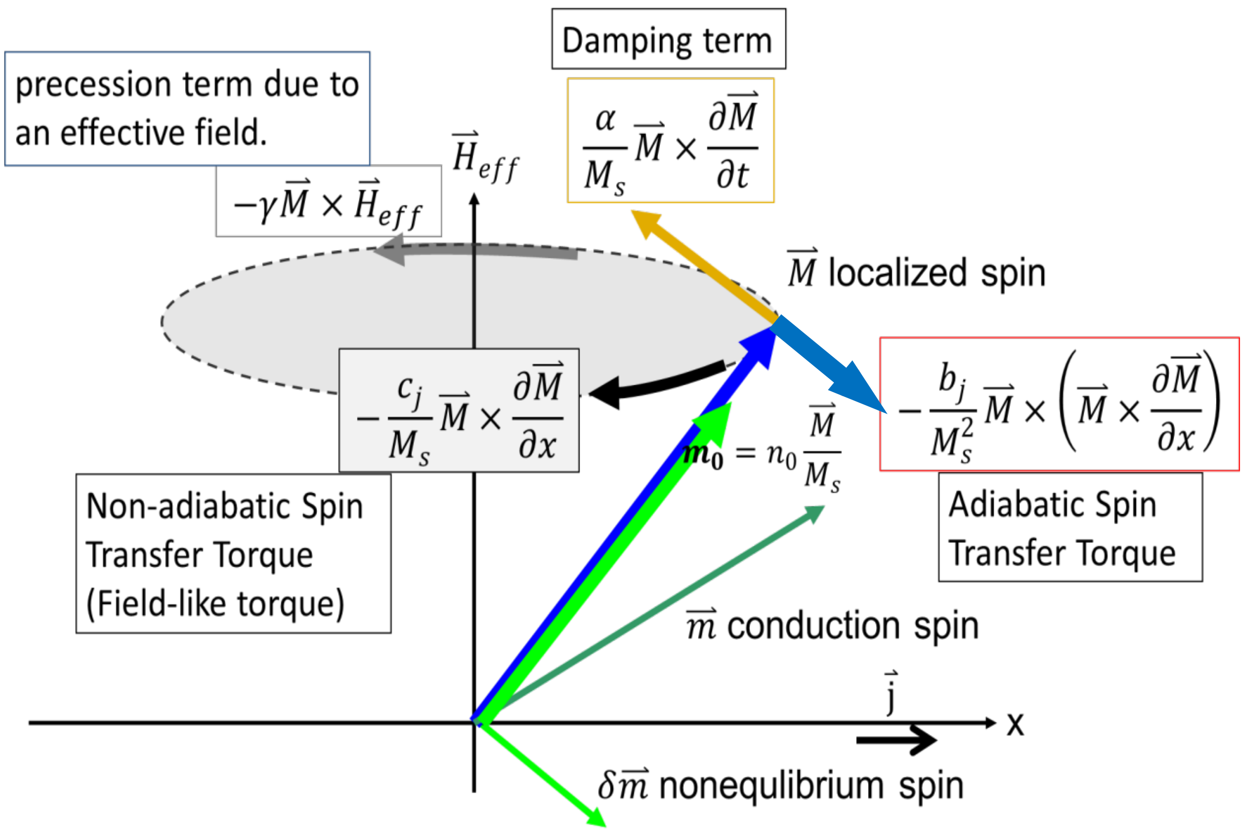

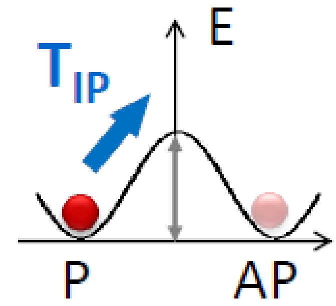

In-plane torque

Anti-damping

Destabilizes M

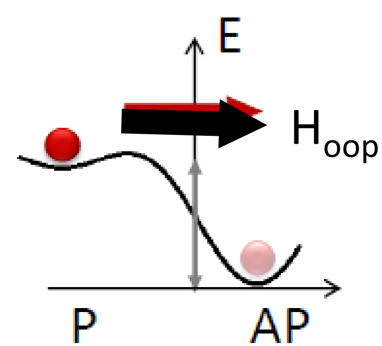

Out-of-plane torque

Field-like torque

Modifies energy barrier

Pure Spin Current

-- with no accompanying net charge current

- Theoretically

$$J_S = \hat{s} \cdot \vec{v} \qquad \rightarrow \qquad J_S = \frac{d}{dt}(\hat{s} \cdot \vec{r}) = \hat{s} \cdot \vec{v} + \frac{d}{dt}\hat{s} \cdot \vec{r}$$

- Experimentally
  - Spin Hall, Inverse Spin Hall effects
  - Spin Pumping effect
  - Spin Seebeck effect

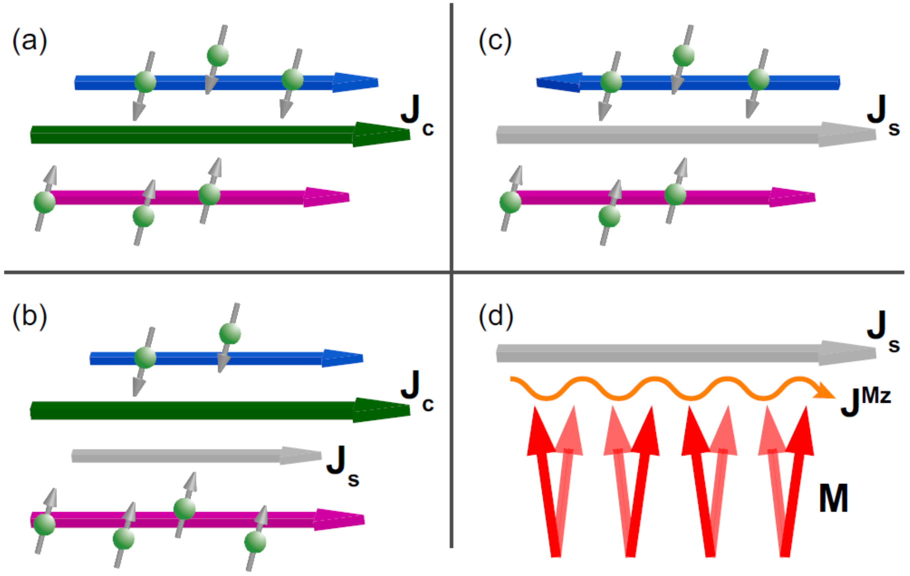

Spin Hall effect

Spin Hall Effect: Electron flow generates transverse spin current

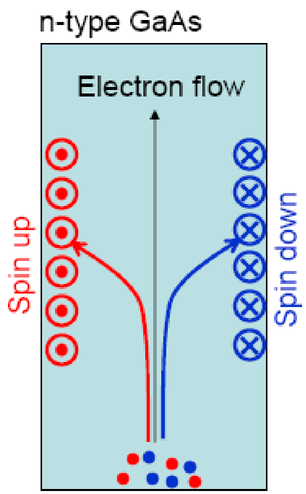

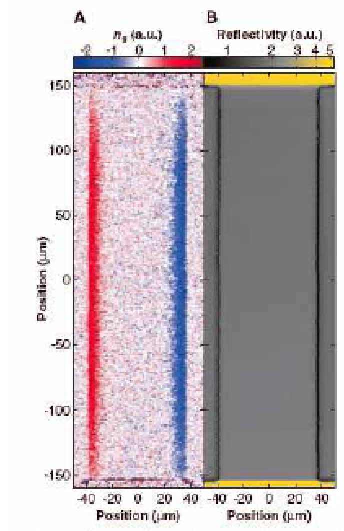

SHE observed in GaAs using Kerr effect to measure spin

Kato et.al. (Awschalom), Science 306, 1910 (2004)

M. I. Dyakonov and V. I. Perel, *JETP* **13** 467 (1971)

J. E. Hirsch, *Phys. Rev. Lett.* **83** 1834 (1999)

Guo *et al*, PRL **100** 096401 (2008)

Now observed at room temperature in ZnSe

The Intrinsic SHE is due to topological band structures

Berry curvature

$$\dot{\vec{r}} = \frac{1}{\hbar}\frac{\partial \varepsilon_n(\vec{k})}{\partial \vec{k}} + \frac{e}{\hbar}\vec{E}\times\vec{\Omega}(\vec{k})$$

The extrinsic SHE is due to asymmetry in electron scattering for up and down spins. – spin dependent probability difference in the electron trajectories

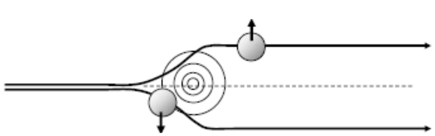

Side jump

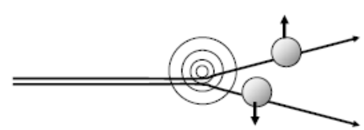

Skew scattering

Spin Pumping

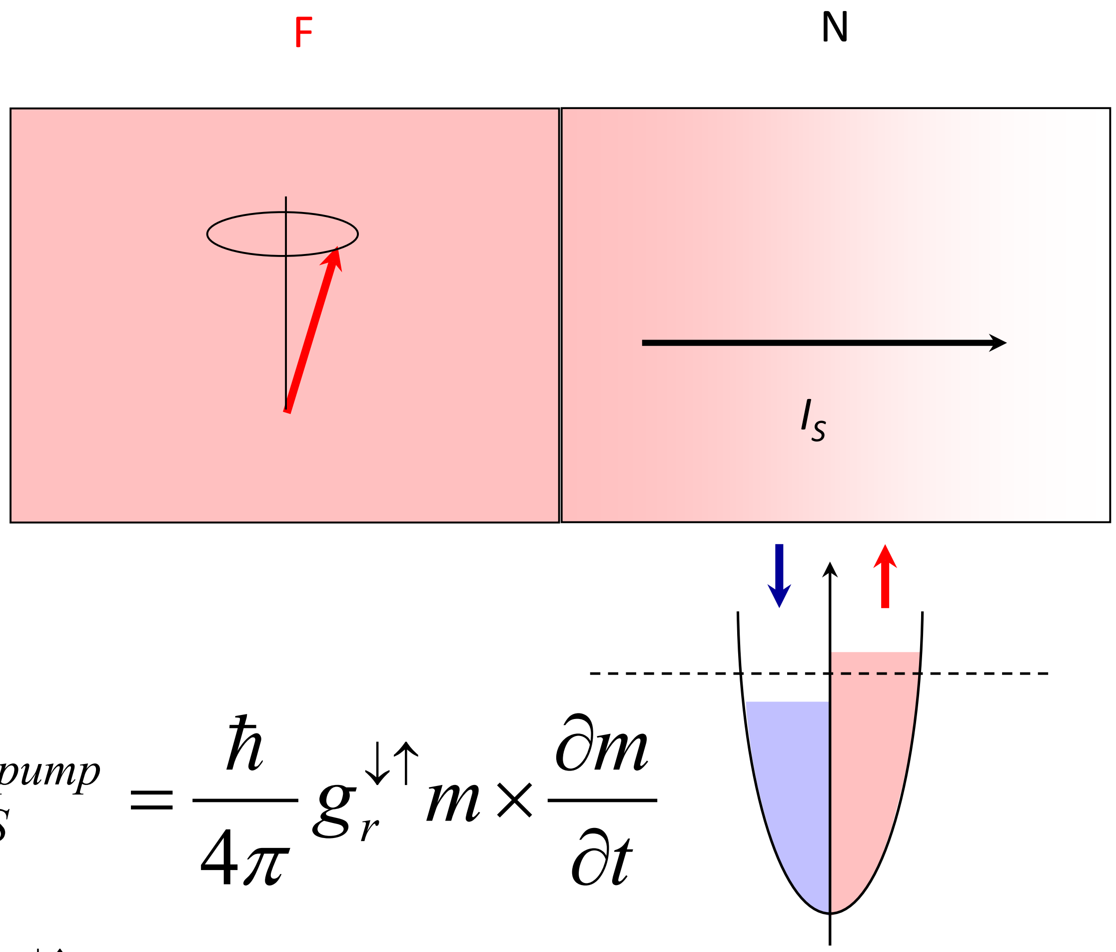

- Landau-Lifshitz-Gilbert

$$\dot{\mathbf{m}} = -\gamma \mathbf{m} \times \mathbf{H}_{\text{eff}} + \mathbf{m} \times (\tilde{\alpha} \dot{\mathbf{m}})$$

$$I_S^{pump} = \frac{\hbar}{4\pi} g_r^{\downarrow\uparrow} m \times \frac{\partial m}{\partial t}$$

$g_r^{\downarrow\uparrow}$: spin mixing conductance

Spin accumulation gives rise to spin current in neighboring normal metal

In the FMR condition, the steady magnetization precession in a F is maintained
by balancing the absorption of the applied microwave
and the dissipation of the spin angular momentum --the transfer of angular momentum from the local spins to conduction electrons, which polarizes the conduction-electron spins.

Spin Seebeck effect

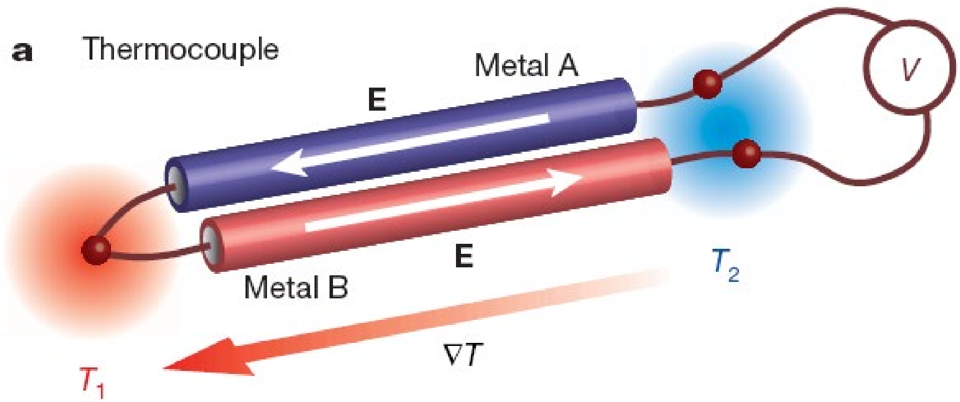

$$\delta V = S\delta T$$

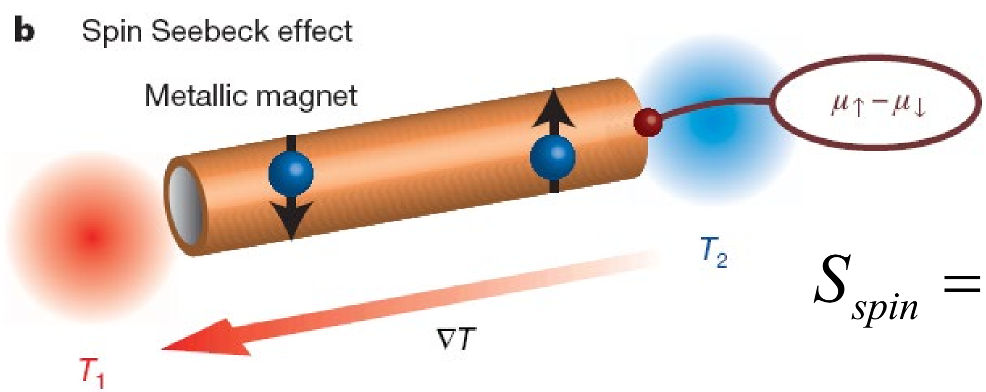

$$\delta V_{spin} = S_{spin}\delta T$$

$$S_{spin} = (1/e)[\partial\mu^{c}{}_{\uparrow}/\partial T - \partial\mu^{c}{}_{\downarrow}/\partial T]$$

Uchida *et al*., Nature **455**, 778 (2008)

Spin Orbit Torque

Landau-Lifshitz-Gilbert equation with Spin Orbit Torque term

$$\frac{\partial \vec{M}}{\partial t} = -\gamma \vec{M} \times \vec{H}_{\text{eff}} + \frac{\alpha}{M_s} \vec{M} \times \frac{\partial \vec{M}}{\partial t} - \frac{b_j}{M_s^2} \vec{M} \times \left(\vec{M} \times \frac{\partial \vec{M}}{\partial x}\right) - \frac{c_j}{M_s} \vec{M} \times \frac{\partial \vec{M}}{\partial x} \qquad b_j, c_j \sim JP/t$$

$$\frac{\partial \mathbf{M}}{\partial t} = -\gamma \mathbf{M} \times \mathbf{H} + \frac{a}{M_s} \mathbf{M} \times \frac{\partial \mathbf{M}}{\partial t} - (\mathbf{u} \cdot \nabla)\mathbf{M} + \frac{\beta}{M_s} \mathbf{M} \times (\mathbf{u} \cdot \nabla)\mathbf{M} + \frac{\alpha_{\text{SHE}}}{M_s} \mathbf{M} \times (\boldsymbol{\sigma} \times \mathbf{M})$$

dissipative and reactive torques

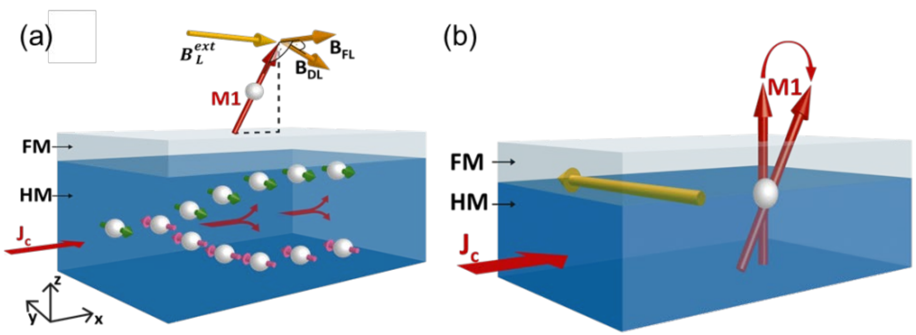

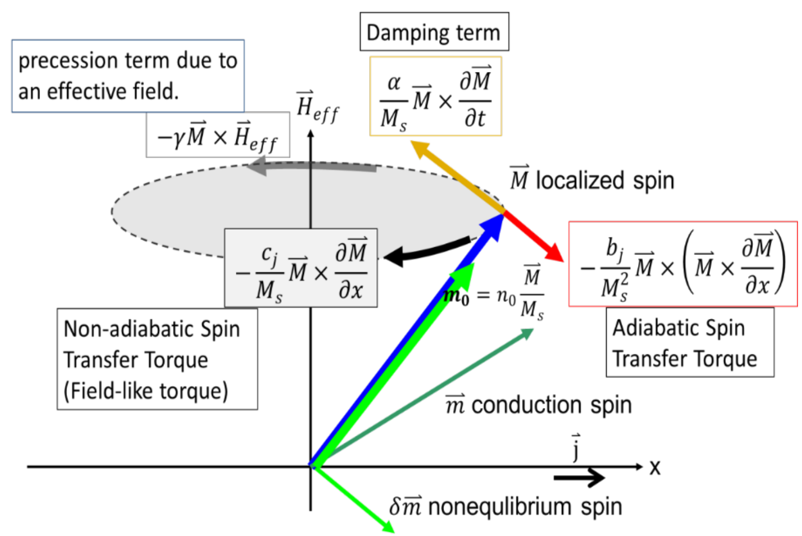

(a) schematics of spin Hall effect. A longitudinal electron current, Jc, in heavy metal (HM) is converted into a transverse spin current by spin-orbit scattering. The spin current leads to a spin accumulation at the HM/FM interface that diffuses across the interface into the FM and exerts torques. (b) The effective field generated by the inverse spin galvanic effect at the interface, which can lead to a switching of the magnetization.

Webpage of **Prof. Dr. Mathias Kläui,** University of Mainz

Spin-orbit torque effect on the Néel vector of an antiferromagnet

The University of Texas at Austin
Department of Physics
College of Natural Sciences

中央研究院物理研究所
INSTITUTE OF PHYSICS, ACADEMIA SINICA

Our works

Collaboration between Academia Sinica and UT Austin

Prof. Shang-Fan Lee

Prof. Xiaoqin Li

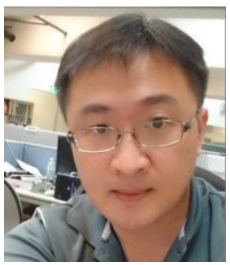

Dr. Liang-Juan Chang

Dr. Ravish K. Jain

Dr. Ngo Trong Hai

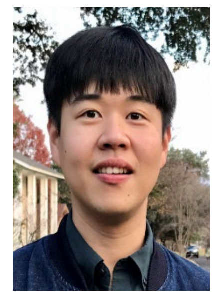

Dongseob Kim

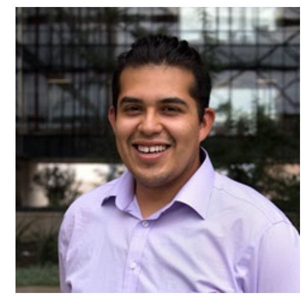

David Lujan

Hung-Yan Chang

Li-Zai Tsai

Yao-Chun Chang

Meng-Tien Chen

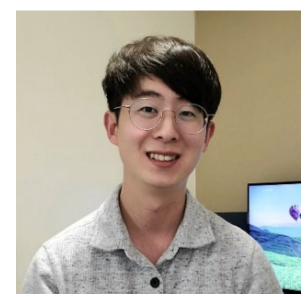

Jeongheon Choe

Magnetic vdW materials offer new opportunities

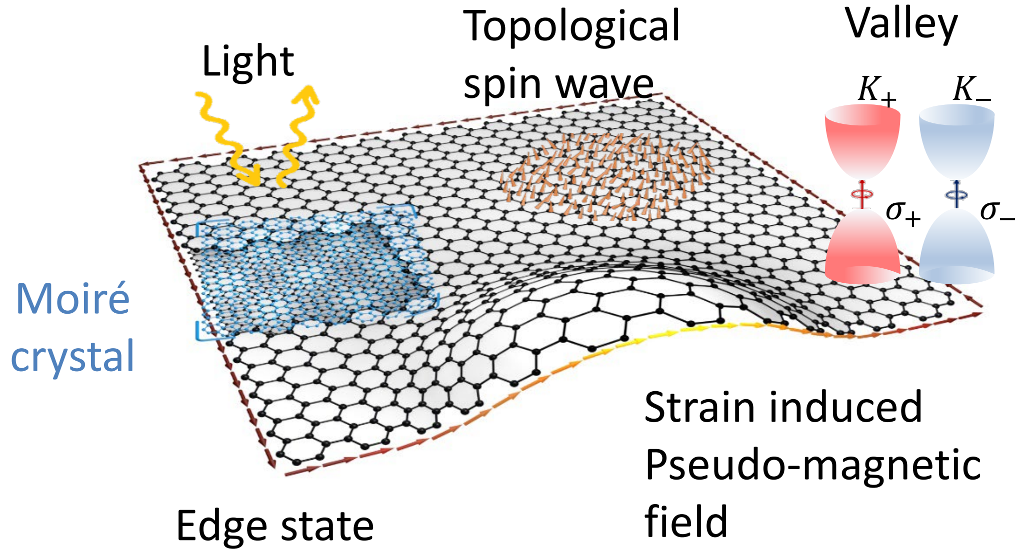

Advantages: precisely defined layer thickness, layer dependent magnetic order, easy to control and easy to integrate with other substrates

van der Waals Antiferromagnets MPS_3

PHYSICAL REVIEW B VOLUME 46, NUMBER 9 1 SEPTEMBER 1992-I

Magnetism in the layered transition-metal thiophosphates MPS_3 (M = Mn, Fe, and Ni)

P. A. Joy and S. Vasudevan
Department of Inorganic and Physical Chemistry, Indian Institute of Science, Bangalore 560 012, India
(Received 22 January 1991; revised manuscript received 3 March 1992)

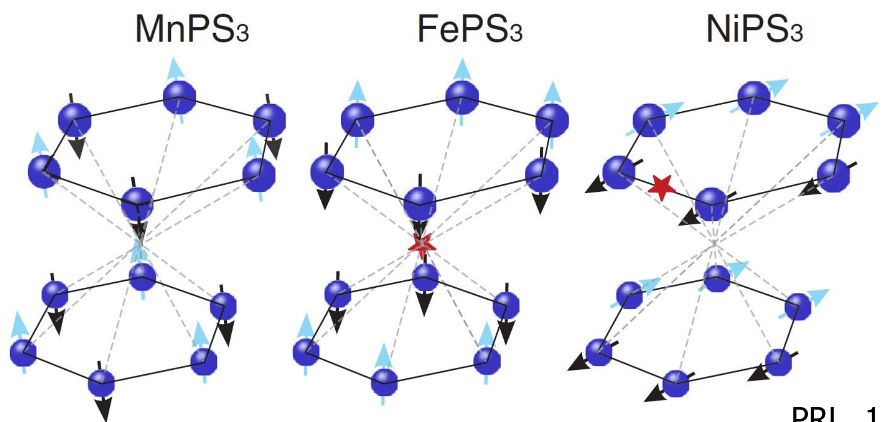

PRL, 124, 027601, 2020

- Honeycomb 2D magnets with a variety of AFM orders
- $MnPS_3$ shows long range AF Neel ordering down to 5.3 nm
- Relatively high transition temperatures, e.g., $NiPS_3$ ~150 K, $FePS_3$ ~118 K, $MnPS_3$ ~78 K

Introduction to $NiPS_3$

- Monoclinic crystal structure with ABAB…. stacking
- Honeycomb lattice within single layer
- Néel Temperature ~155 K
- Magnetic moments in adjacent zig-zag chains are aligned antiparallel.
- Strong third-neighbor antiferromagnetic exchange coupling (J_3)
- Inter-layer spin coupling is ferromagnetic
- Bandgap ~ 1.5 ev – 1.8 eV.
- Ultra sharp, linear polarized PL in AF phase

Spin arrangement and Néel Vector (along a-axis).

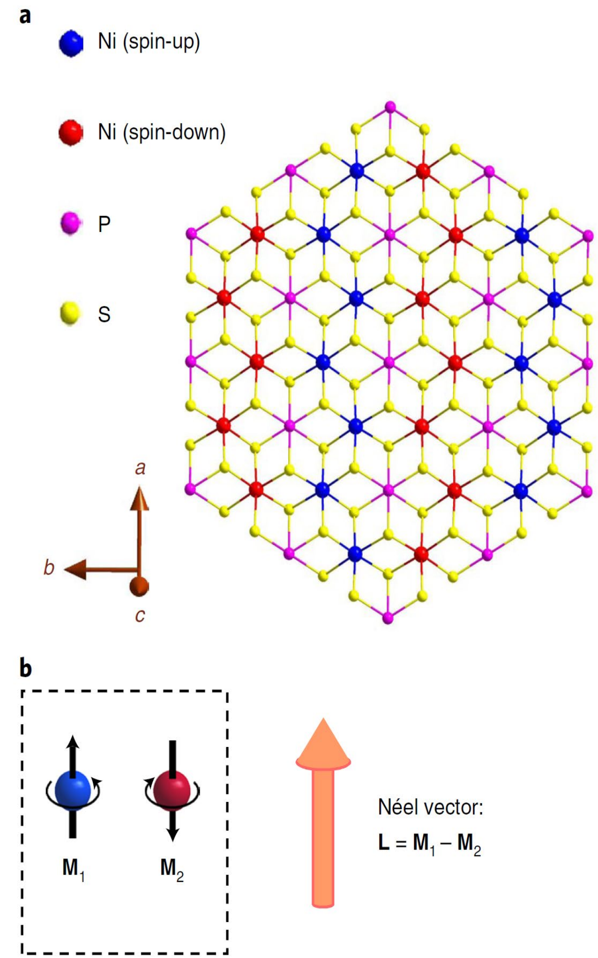

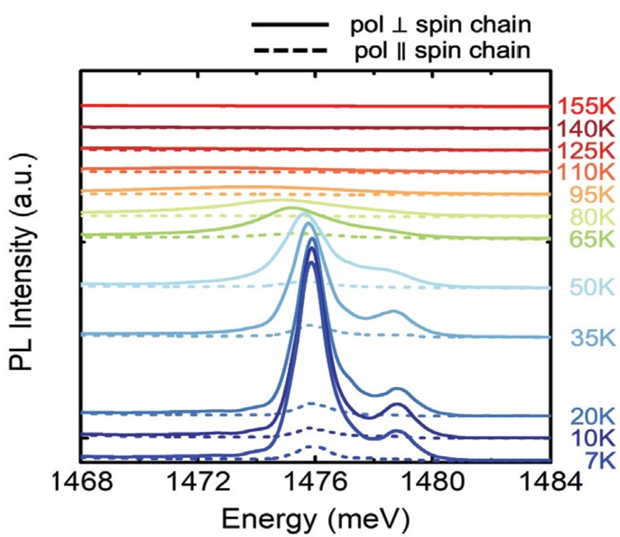

Another visualization of spin arrangement and Néel Vector (along a-axis).

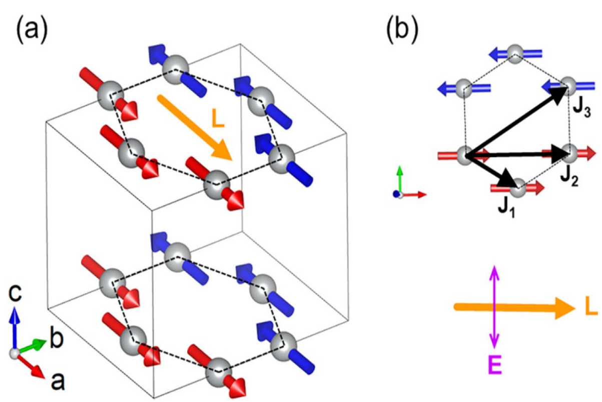

D. S. Kim et al., Adv. Mater., 35 (2023), 2206585
X. Wang et al. Nature Materials 20 (2021) 964–97
D. Jana et al., PRB 108, 115149 (2023)

Ultra sharp Exciton Resonance in $NiPS_3$

Article

Coherent many-body exciton in van der Waals antiferromagnet $NiPS_3$

Nature 583, 785 (2020)

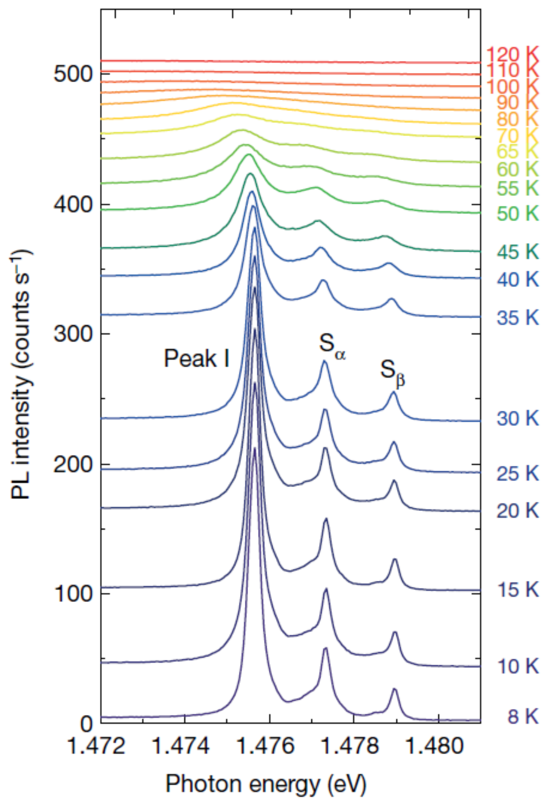

Proposed Zhang-Rice triplet to singlet transition as the mechanism

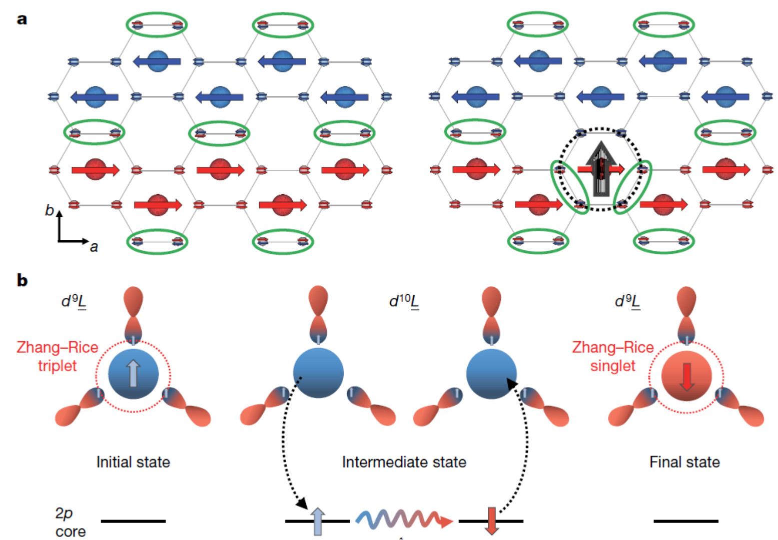

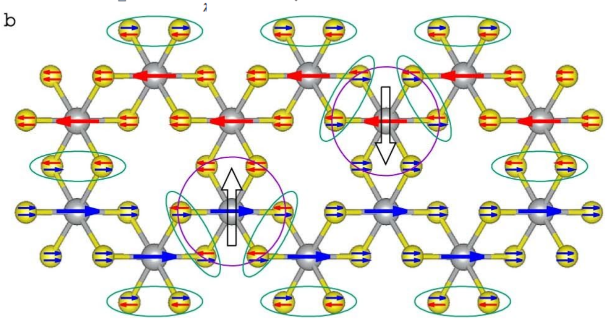

- Identify sharp exciton resonances
- Proposed a mechanism for exciton
- Anisotropic exciton resonances discovered

nature communications

Explore content ⌄ About the journal ⌄ Publish with us ⌄

nature › nature communications › articles › article

Article | Open access | Published: 25 April 2024

Magnetically propagating Hund's exciton in van der Waals antiferromagnet $NiPS_3$

W. He, Y. Shen, K. Wohlfeld, J. Sears, J. Li, J. Pelliciari, M. Walicki, S. Johnston, E. Baldini, V. Bisogni, M. Mitrano & M. P. M. Dean

Nature Communications **15**, Article number: 3496 (2024) | Cite this article

The electronic character, mobility, and magnetic interactions of the exciton remain unresolved. Ultra-high energy resolution resonant inelastic x-ray scattering (RIXS) find that Hund's exchange interactions are primarily responsible for the energy of formation of the exciton.

Measuring the dispersion of the Hund's exciton reveals that it propagates in a way analogous to a double-magnon. Fundamental similarities between the $NiPS_3$ exciton hopping and spin exchange processes, underlining the unique magnetic characteristics of this novel quasiparticle.

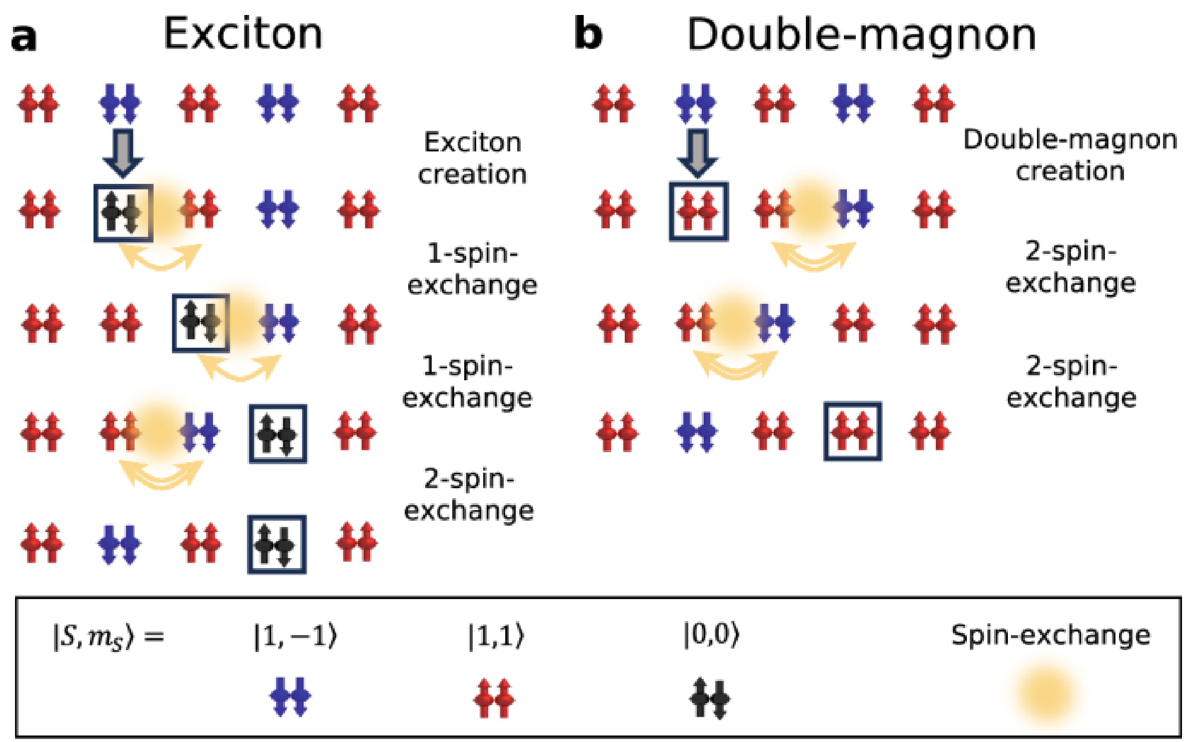

Spin-induced linear polarization of photoluminescence in antiferromagnetic van der Waals crystals

Wang et. al. Nat. Mat. 20, 964, 2021

- Is it the spin chain direction or Neel vector responsible for the polarization direction?
- In this paper, two samples with a axis direction differs by 120º are located. PL polarization is measured with increasing B.
- When B < 9 T, polarization angle is roughly linear with B. 30º ~ 9T

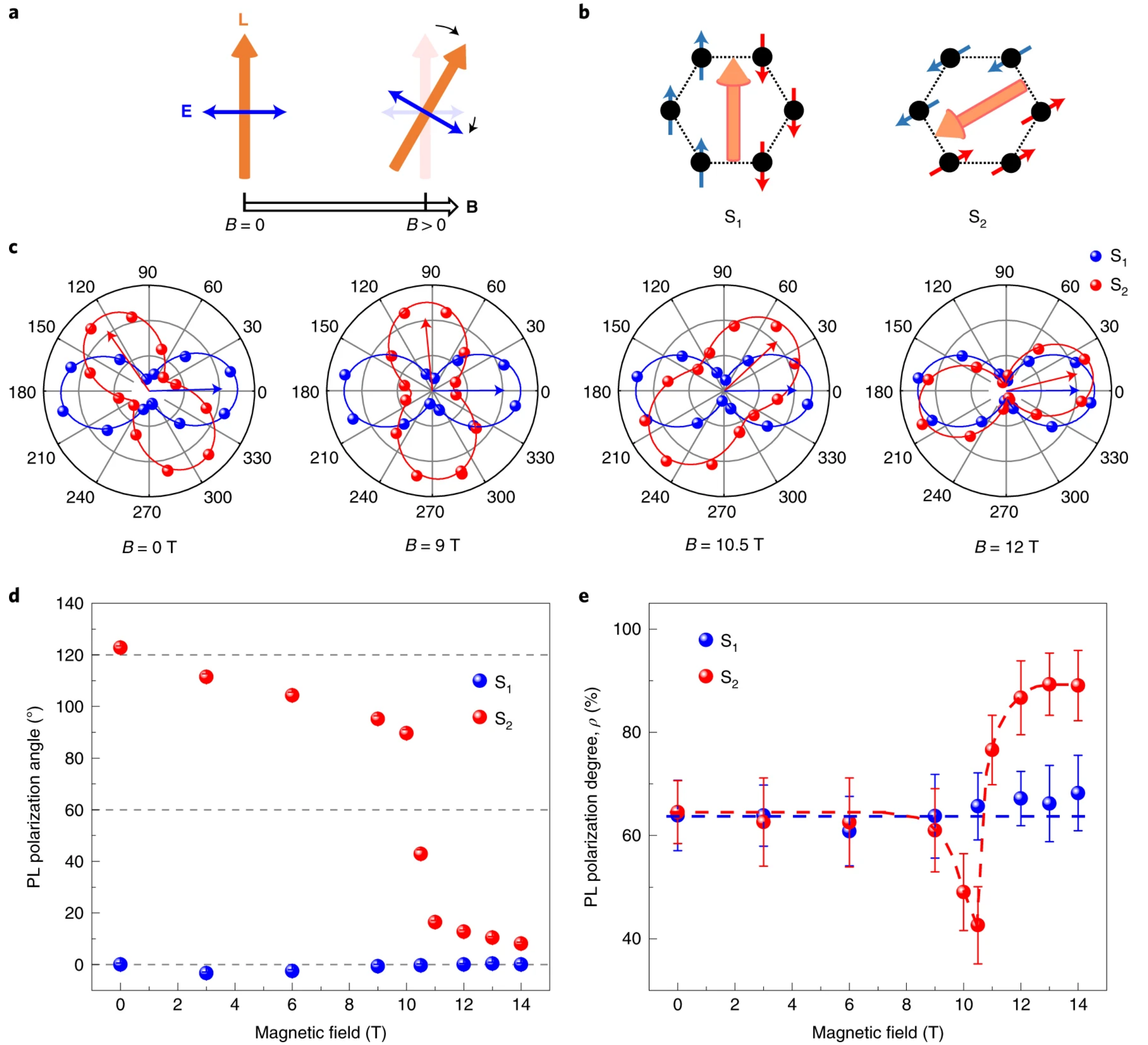

Our study finds something new

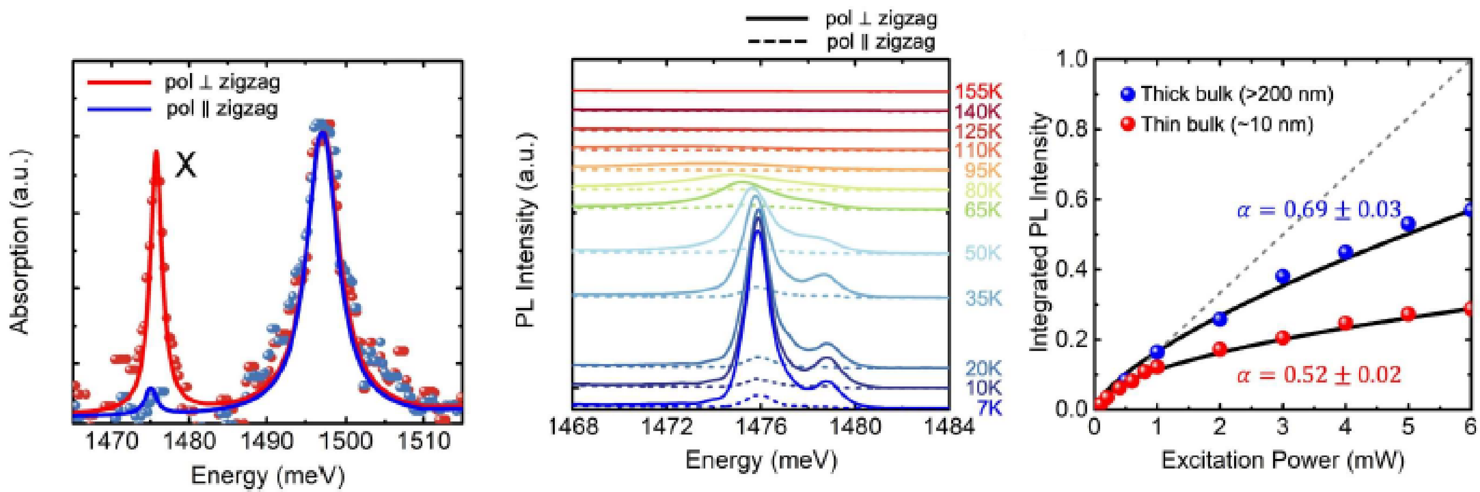

- Exciton induced polarized PL not observed in every sample
- Saturation with excitation power
- PL intensity does not correlated with layer thickness in thin bulks
- Defects?

ADVANCED MATERIALS

Research Article | Full Access

Anisotropic Excitons Reveal Local Spin Chain Directions in a van der Waals Antiferromagnet

Dong Seob Kim, Di Huang, Chunhao Guo, Kejun Li, Dario Rocca, Frank Y. Gao, Jeongheon Choe, David Lujan, Ting-Hsuan Wu, Kung-Hsuan Lin, Edoardo Baldini, Li Yang, Shivani Sharma, Raju Kalaivanan, Raman Sankar, Shang-Fan Lee, Yuan Ping, Xiaoqin Li ... See fewer authors

First published: 27 February 2023 | https://doi.org/10.1002/adma.202206585 | Citations: 3

Dong Seob Kim et. al. Advanced Materials, 2206585, 2023

Three spin chain directions

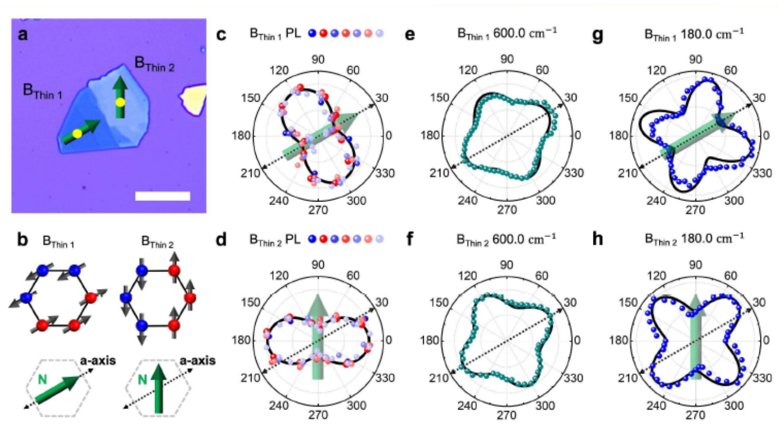

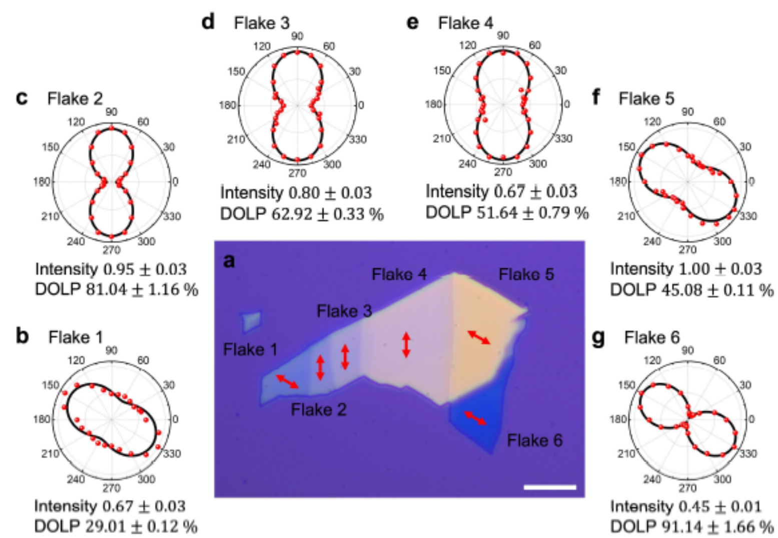

- PL rotations observed on different flakes
- 3 spin chain directions observed: contrary to neutron scattering
- Crystalline axes confirmed via Raman: modes with/without coupling to magnetic order

- Degree of polarization varies spatially
- Coupled vacancies exhibit high degree of polarization
- The value dependent on measurements details and may not reflect intrinsic properties

Electrical detection of the AFM Neel vector

uniaxial collinear antiferromagnetic insulator

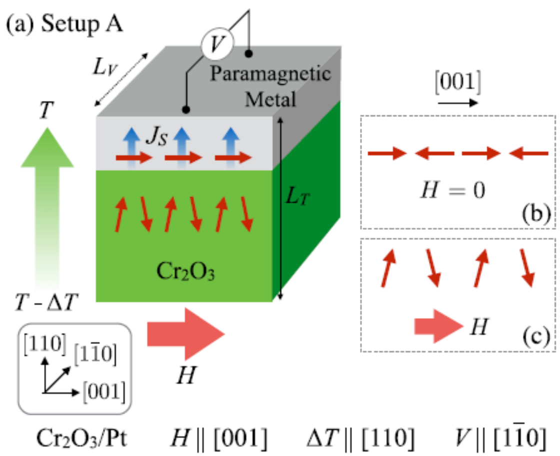

Cr_2O_3

Seki et. al. PRL **115**, 266601 (2015)

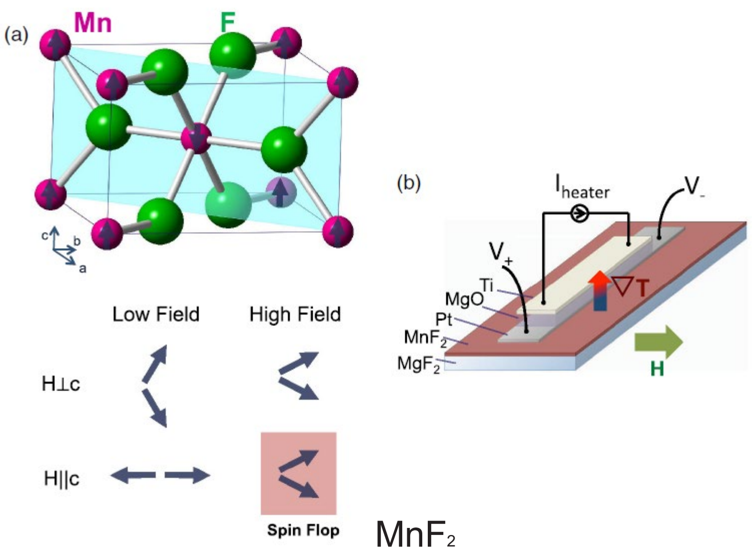

MnF_2

Wu et. al. PRL **116**, 097204 (2016)

Detection of Neel vector spin-flop with increasing magnetic field using thermally induced spin current.
Spin Seebeck + inverse spin Hall effect.

Electrical manipulation and detection of the AFM Neel vector

α-Fe_2O_3, isotropic collinear antiferromagnet

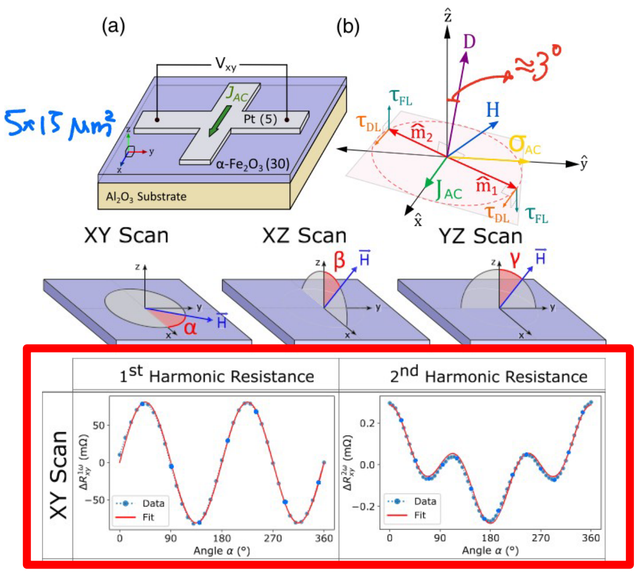

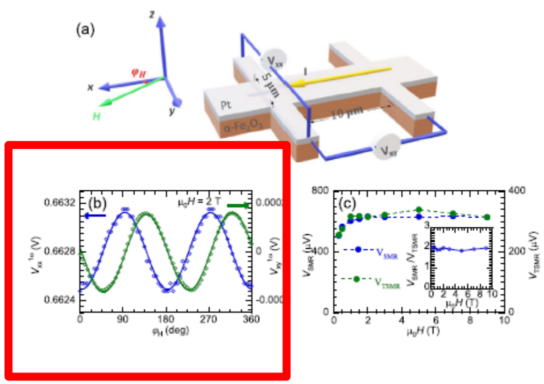

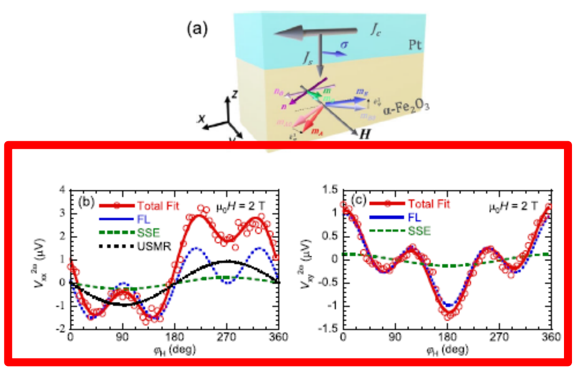

Expected results if Neel vectors are rotated

Quantifying Spin-Orbit Torques in Antiferromagnet–Heavy-Metal Heterostructures
Cogulu et al., Phys. Rev. Lett. **128**, 247204 (2022)

Unidirectional Spin Hall Magnetoresistance in Antiferromagnetic Heterostructures
Cheng et al., Phys. Rev. Lett. **130**, 086703 (2023)

Electrical manipulation and detection of the AFM Neel vector

Manipulation of collinear antiferromagnet Neel vector by electrical pulses in conducting materials

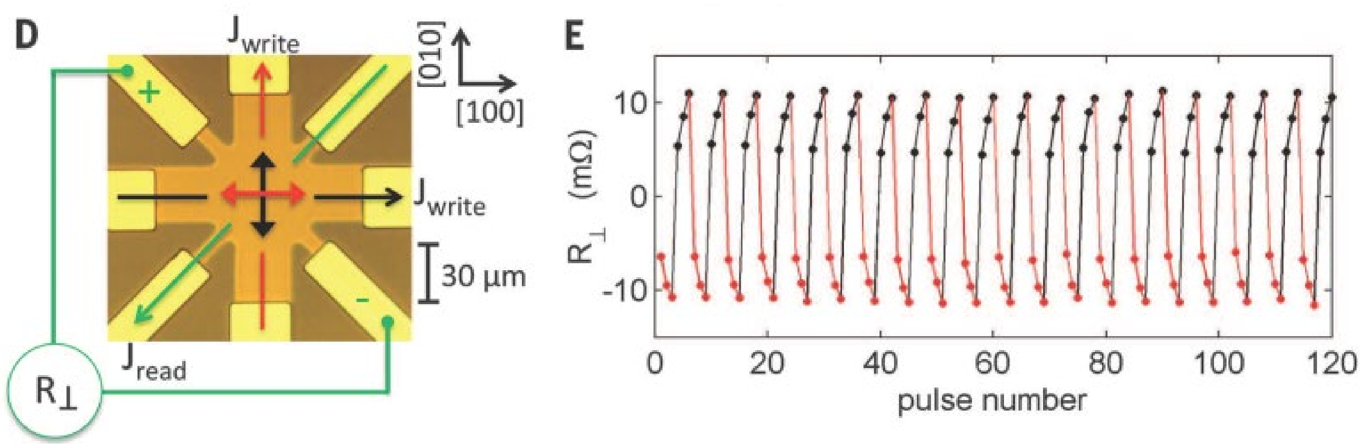

P. Wadley et al, Science, 2016

- Material: CuMnAs
- Pass three consecutive pulses in two directions (red and black) → Measure the hall resistance
- Hall resistance indicates the spin chain direction

Extension of analytical model to include uniaxial anisotropy in AFM

The AFM dynamics can be described by the Landau–Lifshitz–Gilbert–Slonczewski (LLGS) equation

$$\frac{d\boldsymbol{S}_i}{\gamma dt} = \boldsymbol{H}_{\text{eff},i} \times \boldsymbol{S}_i + (\boldsymbol{H}_D \times \boldsymbol{S}_i) \times \boldsymbol{S}_i,$$

$$\boldsymbol{n} \times \left\{ \frac{1}{2H_E} \left[-\frac{\partial^2 \boldsymbol{n}}{\partial t^2} - \frac{\partial \boldsymbol{n}}{\partial t} \times \boldsymbol{H_t} + \frac{\partial}{\partial t} (\boldsymbol{H_t} \times \boldsymbol{n}) - \boldsymbol{D}\hat{z} (\boldsymbol{D}\hat{z} \cdot \boldsymbol{n}) - \boldsymbol{D}\hat{z} \times \boldsymbol{H_t} - (\boldsymbol{n} \cdot \boldsymbol{H_t}) \boldsymbol{H_t} \right] - 2H_\perp (\boldsymbol{n} \cdot \hat{z}) \hat{z} + 2H_\parallel (\boldsymbol{n} \cdot \hat{a}) \hat{a} \right\} = \boldsymbol{n} \times (\boldsymbol{n} \times \boldsymbol{H_D}).$$

$$\boldsymbol{n} \times \left(-\frac{\partial^2 \boldsymbol{n}}{\partial t^2} - 2\frac{\partial \boldsymbol{n}}{\partial t} \times \boldsymbol{H} + \boldsymbol{A}\boldsymbol{n} \right) = 0$$

where $\boldsymbol{A} = -\boldsymbol{H} \otimes \boldsymbol{H} - 4H_E H_\perp \hat{z} \otimes \hat{z} + 4H_E H_\parallel \hat{x} \otimes \hat{x}$ is a 3 by 3 matrix, explicitly:

$$\boldsymbol{A} = \begin{bmatrix} 4H_E H_\parallel - H_x^2 & -H_x H_y & -H_x H_z \\ -H_x H_y & -H_y^2 & -H_y H_z \\ -H_x H_z & -H_y H_z & -4H_E H_\perp - H_z^2 \end{bmatrix}$$

Hall voltage response could be expand as:

$$V_H(t) = R_H(0) I_0 \cos\omega t + \frac{1}{2} \frac{\partial R_H}{\partial I}\bigg|_{I=0} I_0^2 (1 + \cos 2\omega t) = V_0 + V_{1\omega} \cos\omega t + V_{2\omega} \cos 2\omega t$$

$$V_{1\omega} = \frac{1}{2} I_0 R_0 \sin(2\phi_n)$$

$$V_{2\omega}^{SOT} = -\frac{H_F}{4H} \frac{\cos(\phi_H) + \cos(\phi_H - 4\phi_n)}{\alpha \cos(2\phi_a - 2\phi_n) - \cos(2\phi_H - 2\phi_n)} I_0 R_0$$

Hung-Yan Chang

Journal of Magnetism and Magnetic Materials 556 (2022) 169362

Contents lists available at ScienceDirect

ELSEVIER

Journal of Magnetism and Magnetic Materials

journal homepage: www.elsevier.com/locate/jmmm

Research article

Theory of harmonic Hall responses of spin-torque driven antiferromagnets

Hantao Zhang[a], Ran Cheng[a,b,*]

Zhang and Cheng, JMMM 556, 169362 (2022)

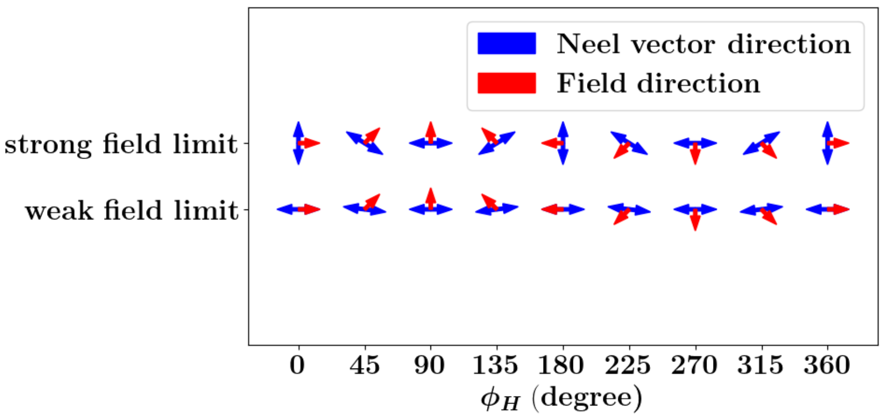

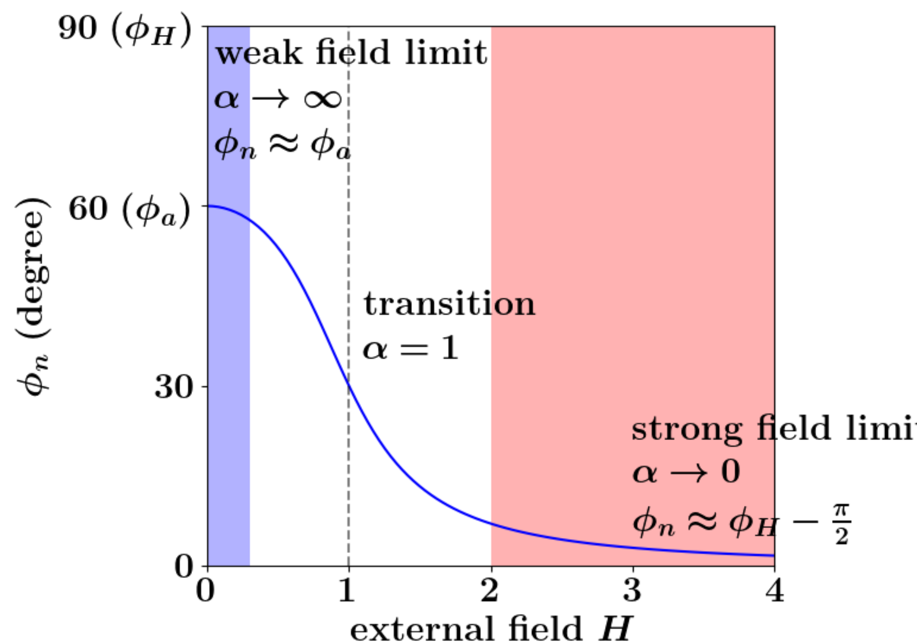

$\alpha = 4H_{\parallel}H_E/H^2$ is the spin-flop field, denotes the relative strength between the in-plane anisotropy and the external field.

Take-home messages

- In NiPS3, anisotropic excitons reveal local Neel vector directions
- 3 polarized directions observed: contrary to neutron scattering
- Weak interlayer coupling leads to 3 polarized PL directions despite the bulk monoclinic crystals
- A different exciton formation mechanism proposed
- Questions: Is the magnetic order stable in the monolayer limit where three three directions should be energetically degenerate?
- Theoretical model is extended to include in-plane uniaxial anisotropy
- Derived spin-flop field formula works quantitatively for NiO and NiPS3
- First and second harmonic Hall voltages due to spin orbit torque are derived and used to explain experimental data on NiPS3
- Spin orbit torque has the same order of magnitude contribution as spin Seebeck effect in NiPS3/Pt heterostructure

Acknowledgements

Financial supports from Academia Sinica and NSTC, NSTC-USAF, project grant no.: 110-2124-M-001-009-MY3 are acknowledged.